Interaction between soot and stored NO$_x$ during operation of LNT Pt–Ba/Al$_2$O$_3$ catalysts

Roberto Matarrese, Nancy Artioli, Lidia Castoldi, Luca Lietti*, Pio Forzatti

Dipartimento di Energia, Laboratory of Catalysis and Catalytic Processes and NEMAS, Centre of Excellence, Politecnico di Milano, P.zza L. da Vinci 32, Milano, Italy

ABSTRACT

The interaction of soot with nitrates stored on a model PtBa/Al$_2$O$_3$ LNT catalyst sample is here investigated under realistic conditions, i.e. upon lean/rich cycling in the presence of water and CO$_2$. The presence of soot inhibits the NO$_x$ storage capacity of the catalyst during the lean phase at different temperatures, in the range 200–350 °C, but does not affect significantly the regeneration process of the stored nitrates. Simultaneously with the NO$_x$ storage, soot is converted to CO$_2$ at temperatures above 300 °C. Soot is oxidized by NO$_2$ formed by NO oxidation on Pt sites, but the participation of the stored nitrates in the soot oxidation is also likely, as pointed out by TPD/TPO experiments showing the occurrence of a surface reaction involving soot and the stored nitrates.

© 2011 Elsevier B.V. All rights reserved.

1. Introduction

The reduction of both soot (particulate matter) and NO$_x$ emissions from diesel-equipped vehicles is nowadays mandatory to cope with the next coming emission standards [1]. The soot removal relies on the use of diesel particulate filters (DPFs) [2], that must be periodically regenerated to remove the entrapped soot avoiding excessive pressure drops at the exhaust. For this reason the filter may by catalyzed to promote soot combustion at lower temperatures.

Concerning NO$_x$, either selective catalytic reduction (SCR) [3,4] or nitrogen storage reduction (NSR), also quoted as lean NO$_x$ trap (LNT) [5–7], represent the top contenders for reducing NO$_x$ concentrations in the exhausts from diesel and lean burn gasoline engines [1]. While the SCR technique is based on the reaction between injected NH$_3$ and NO present in the flue gases on metal-substituted zeolites [1] or vanadia–tungsta–titania catalysts [8], NSR catalysts make no use of any external reductant. These catalysts operate the NO$_x$ reduction under cyclic conditions by alternating long lean phases during which NO$_x$ emitted in the exhaust gases are adsorbed on the catalyst, with subsequent short rich periods in which the stored NO$_x$ are reduced by H$_2$, CO and hydrocarbons (HC) present in the flue gases to produce nitrogen [5–7]. LNT catalysts are generally made by a high surface area support (such as γ-Al$_2$O$_3$),

alkaline/alkaline-earth metal oxides (such as K$_2$O and BaO) and precious metals like Pt, Rh, Pd; other components are also present in fully formulated catalysts (e.g. CeO$_2$). Hybrid NSR + SCR configurations have also been proposed, since they guarantee higher NO$_x$ removal efficiencies [3,9–14].

Exhaust after-treatment systems able to cope with the next coming strict emission standards are rather complex. De-soot and De-NO$_x$ devices are used, along with a diesel oxidation catalyst (DOC) as well. However the optimal design of the after treatment exhaust system is still a matter of debate: the DOC is generally placed upstream the DPF and SCR/LNT converters, while different solutions have been proposed for the DPF and the DeNO$_x$ catalyst. Integrated (or one-pot) solutions have been proposed, like catalyzed diesel particulate filters (CDPFs) which act as DOC but also remove soot, or the DPNR (diesel particulate-NO$_x$ reduction) technology which has been recently proposed by the Toyota group [15,16]. The DPNR technique has the unique capacity to remove simultaneously soot and NO$_x$, and is based on the use of a catalyzed filter on which a NSR catalyst is deposited. In this way soot is removed by the filter while NO$_x$ are reduced according to the NSR technology [15].

Despite DPNR systems are used at a commercial scale, still many aspects concerning their catalytic performances, the operating reaction mechanisms and the interactions between the De-soot and De-NO$_x$ functions are still under debate. This has motivated in recent years a number of studies concerning the reactivity of NSR catalysts in the presence of soot [17–20]. In previous works from our group the behavior of model PtBa/Al$_2$O$_3$ and PtK/Al$_2$O$_3$

LNT catalysts in the simultaneous removal of soot and NO_x has been investigated. It has been shown that during the lean phase NO_x are being stored on the catalyst surface, while soot oxidation occurs involving primarily NO_2, formed upon NO oxidation [21,22]. However more recent studies have shown that NO_x species, stored onto the trapping component of the catalyst, may participate in the combustion of soot by releasing gaseous NO_x upon decomposition and/or by directly reacting with soot according to a surface reaction [23–26]. Besides, it has been shown that the presence of soot depresses the NO_x storage capacity of the catalyst, in line with data obtained by Pieta et al. [27].

Along similar lines, Kustov et al. [18] showed that the stored nitrates may decrease the temperature of soot oxidation when nitrate decomposition occurs in a proper temperature range, due to the release of NO_2 in the gas phase. More recently studies carried out by Sanchez et al. [28,29] on K/La_2O_3-based catalysts indicated that the reaction between soot and trapped NO_x can proceed before the decomposition of nitrates.

Aim of the present work is to provide additional insights on the effects of the presence of soot on the catalytic behavior of a model $PtBa/Al_2O_3$ LNT catalyst, and in particular to gain further insight on the interaction between soot and the stored NO_x on the De-soot and De-NO_x activity of the catalyst. For this purpose, NO_x storage/reduction experiments have been performed over the selected catalyst sample by alternating lean/rich cycles both in the presence and in the absence of soot. At variance with previous studies [21–23,25,26], in this study the absorption and reduction of the NO_x has been investigated by alternating short lean and rich phases with no inert purge in between, thus providing results closer to the transient conditions adopted under real applications.

The interaction between soot and the stored NO_x species has been further investigated by temperature programmed methods under inert flow (TPD) and in the presence of oxygen (TPO) in which the stability/reactivity of the stored NO_x species has been analyzed both in the presence and in the absence of soot. The experiments have also been carried out over a platinum-free catalyst in order to assess the role of Pt in the stability/reactivity of adsorbed nitrates as well.

2. Materials and methods

A model $PtBa/Al_2O_3$ (1/20/100 w/w/w) catalyst was used in this study. The sample was prepared by incipient wetness impregnation with dinitro-diammine platinum (Strem Chemicals, 5%) and then with barium acetate of an Al_2O_3 support, obtained by calcination at 700 °C of a commercial alumina (Versal 250 from UOP). After each impregnation steps, the powders was dried overnight in air at 80 °C and calcined at 500 °C for 5 h. The selected impregnation order (first Pt and then Ba) has been adopted in order to ensure a good dispersion and stability of the noble metal on the alumina support, in line with the recipes of Toyota patents [30]. A Pt-free sample (Ba/Al_2O_3, 20/100 w/w) was also prepared by impregnation of alumina with an aqueous solution of barium acetate (Sigma–Aldrich, 99%), followed by drying overnight in air at 80 °C and calcination at 500 °C for 5 h. Finally, for comparison purposes, a sample was also prepared in which a $Ba(NO_3)_2$ solution was directly impregnated over the calcined alumina support (Ba/Al_2O_3 ratio: 20/100 w/w). After impregnation, the sample was dried at 80 °C overnight. In the following, this sample will be referred as $Ba(NO_3)_2/Al_2O_3$.

Surface area and pore size distribution of the prepared catalyst samples were determined by N_2 adsorption–desorption with the BET method using a Micromeritics TriStar 3000 instrument. The specific surface area of the ternary $PtBa/Al_2O_3$ sample is near $160 \, m^2 \, g^{-1}$; a lower surface area value was determined for the Ba/Al_2O_3 sample ($105 \, m^2 \, g^{-1}$). The surface area contraction

is accompanied by a slight reduction of the pore volume, from $0.80 \, cm^3/g$ for the $PtBa/Al_2O_3$ catalyst down to $0.63 \, cm^3/g$ for the binary Ba/Al_2O_3 sample. The Pt dispersion of the $PtBa/Al_2O_3$ sample was also estimated by hydrogen chemisorption at 0 °C (TPD/R/O 1100 Thermo Fischer Instrument). The measured Pt dispersion value was near 60%.

The Ba/Al_2O_3 and $PtBa/Al_2O_3$ catalysts were characterized by XRD analysis (Brüker D8 Advanced Instrument equipped with graphite monochromator on the diffracted beam). The XRD patterns showed both the monoclinic (JCPDS 78-2057) and orthorhombic (Whiterite, JCPDS 5-378) polymorphic forms of $BaCO_3$, in addition to microcrystalline γ-Al_2O_3 (JCPDS 10-425).

Printex-U (Degussa) was used as model soot, whose properties are well addressed in the literature [31]. Catalyst-soot mixtures were prepared by gently mixing in a vial the catalyst powder (74–105 μm) with the soot, thus realizing a loose contact which is representative of the soot/catalyst contact mode occurring in the DPNR system where soot is entrapped in the filter pores [15]. A soot loading (w_{soot}/w_{cat}) near 11% has been typically employed. A sample with an intimate catalyst/soot interaction was also prepared by direct impregnation of the soot powder with aqueous solutions of Ba nitrate ("full contact" sample [32]). After impregnation, the sample was dried overnight at 100 °C. In the following, this sample will be referred to as $Ba(NO_3)_2/soot$.

The reactivity experiments were performed in a flow microreactor system, consisting of a quartz tube (7 mm i.d.) equipped with a mass spectrometer (Omnistar 200, Pfeiffer Vacuum), a micro GC (Agilent 3000A) and an UV analyzer (Limas 11HW, ABB) for the on-line analysis of the reaction products. In each run 60 mg of catalyst have been used and the total flow rate was set at $100 \, cm^3/min$ (at 0 °C and 1 atm). The catalytic De-NO_x and De-soot activity was investigated by performing lean–rich cycles at constant temperature alternating rectangular step feeds of NO (1000 ppm, v/v) + 3% (v/v) of O_2 (lean phase) with feeds of H_2 (4000 ppm, v/v, rich phase). The abrupt switches between the adsorption and the regeneration phase have been realized with the use of four-port valves. Experiments were performed in presence of 1% (v/v) H_2O and 0.1% (v/v) CO_2 at different temperatures, in the range 200–350 °C and with different NO inlet concentrations (500, 1000 ppm).

In order to analyze the interaction between soot and the stored NO_x, TPD and TPO experiments were also performed over $PtBa/Al_2O_3$ and Ba/Al_2O_3 catalysts. Accordingly NO_x have been stored onto the catalytic surface in the absence of soot at 350 °C with NO or NO_2 (1000 ppm, v/v) in He + O_2 (3%, v/v) + H_2O (1%, v/v) + CO_2 (0,1%, v/v); then the catalyst has been cooled at room temperature in He, extracted from the reactor and mixed with soot (11%, w/w). TPD and TPO experiments have been carried out by heating the so-prepared catalyst-soot mixture at a rate of 10 °C/min in He + H_2O (1%, v/v) + CO_2 (0.1%, v/v) in the absence and in the presence of 3% (v/v) O_2, respectively, from room temperature to 500 °C. The results collected with the catalyst/soot mixture have been compared with those obtained in analogous experiments performed in the absence of soot. TPD experiments have also been performed over $Ba(NO_3)_2/Al_2O_3$ (with and without soot) and over the "full contact" $Ba(NO_3)_2/soot$ system.

3. Results and discussion

3.1. NO_x storage/reduction cycles in the presence of soot

In order to study the effect of soot on the catalyst activity in the NO_x adsorption and reduction, lean–rich cycles have been performed in the presence of soot over the model $PtBa/Al_2O_3$ NSR sample. Fig. 1 shows a typical result, in terms of NO, NO_2, CO_2, H_2 and N_2 outlet concentration vs. time, of a sequence of four lean–rich
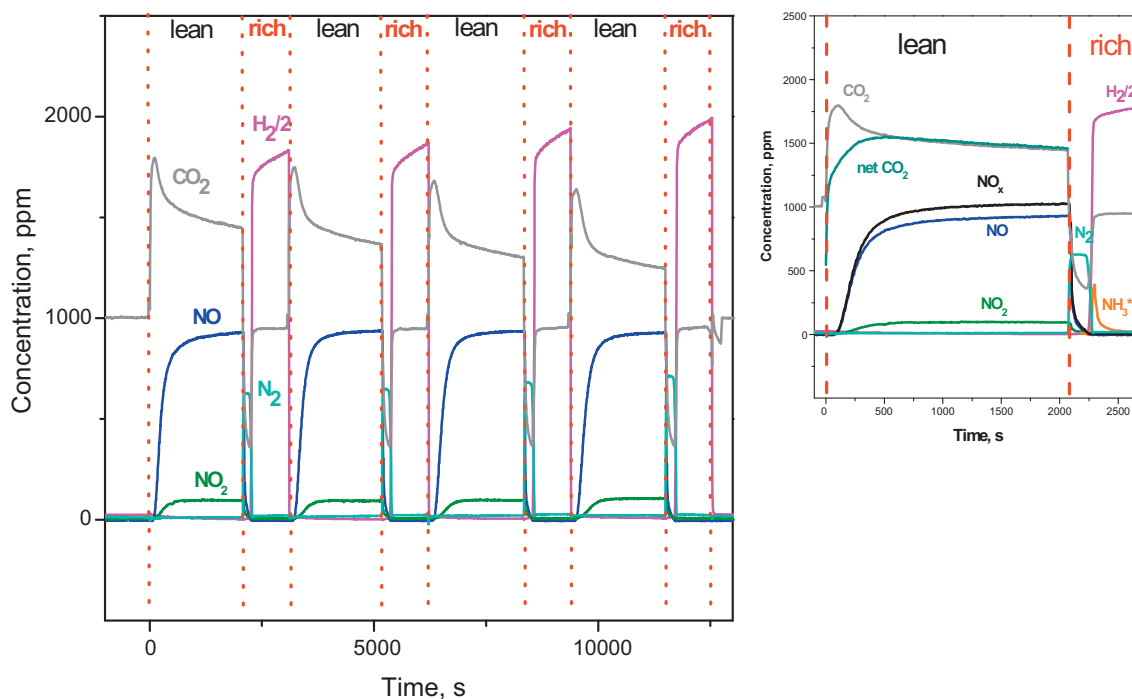
Fig. 1. Lean–rich cycles at 350 °C over PtBa/Al$_2$O$_3$-soot mixture. Only the first cycle is reported in the insert. Lean phase: 1000 ppm NO + O$_2$ (3%, v/v) in He, CO$_2$ (0.1%, v/v) and H$_2$O (1%); rich phase: 4000 ppm H$_2$ in He, CO$_2$ (0.1%, v/v) and H$_2$O (1%).

phases at 350 °C. For the sake of clarity, in the insert of the figure an enlargement of the first cycle of the sequence can be seen, showing the concentrations of NO, NO$_2$, NO$_x$ (=NO + NO$_2$), CO$_2$, H$_2$, N$_2$ and ammonia. Upon NO and O$_2$ admission (at $t = 0$ s, insert of Fig. 1) the NO outlet concentration shows a delay of 100 s, and then increases to a steady level near 930 ppm. Also NO$_2$ formation is observed (with a time delay of 170 s), due to the occurrence of the oxidation of NO by O$_2$ at Pt sites according to the stoichiometry of reaction (1):

$$NO + 1/2O_2 \rightarrow NO_2 \qquad (1)$$

The outlet concentrations of both NO and NO$_2$ increase with time and eventually reach a steady state level, indicating that the maximum NO$_x$ storage capacity of the sample has been reached. The area included between the NO inlet and NO$_x$ outlet concentration traces is proportional to the amount of NO$_x$ that have been stored onto the catalyst surface (4.04 × 10^{-4} mol/g$_{cat}$).

Upon NO admission, the evolution of CO$_2$ is also observed. In fact the CO$_2$ concentration rapidly increases from its background level (1000 ppm) showing a maximum of 1800 ppm and then decreases approaching the constant value of 1450 ppm near the end of the pulse. As already reported elsewhere [21,25,26], the increase in the CO$_2$ outlet concentration results from two factors. One is related to the formation of Ba nitrates at the expenses of Ba-carbonates upon NO$_x$ adsorption, as described by the stoichiometry of reaction (2):

$$BaCO_3 + 2NO + 3/2O_2 \rightarrow Ba(NO_3)_2 + CO_2 \qquad (2)$$
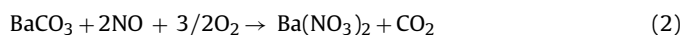
In reaction (2), formation of nitrates only is suggested as NO$_x$ adsorbed species, in line with many studies showing that at this temperature only nitrates are formed upon NO/O$_2$ adsorption [33]. Reaction (2) is responsible for the initial CO$_2$ peak; then the CO$_2$ concentration remains above its background level due to soot combustion. As a matter of fact, by subtracting from the CO$_2$ concentration trace the amounts of CO$_2$ resulting from the NO$_x$ uptake and calculated according to the stoichiometry of reaction (2), a net CO$_2$ concentration trace is obtained (see the insert) which refers uniquely to soot combustion. At the end of the lean phase, the rate

of CO$_2$ formation due to soot combustion is near 3.35 × 10^{-8} mol/s; roughly 13% of the initial soot loading (11%, w/w) is consumed during the first lean/rich sequence. Since no appreciable CO$_2$ formation is seen before the lean–rich cycles, i.e. in the presence of O$_2$ only, NO$_x$ (either adsorbed or in the gas phase) are involved at the temperature of 350 °C in the oxidation of soot, possibly according to the stoichiometry of reactions (3) and (4):

$$NO_2 + C \rightarrow NO + CO \qquad (3)$$

$$CO + 1/2O_2 \rightarrow CO_2 \qquad (4)$$

Here, NO$_2$ formed upon NO oxidation at Pt sites oxidizes soot with formation of CO (and possibly of CO$_2$); CO is then oxidized to CO$_2$ by O$_2$ at Pt sites and/or by NO$_2$. As a matter of facts, studies on the non-catalytic oxidation of soot by NO$_2$/O$_2$ mixtures carried out elsewhere pointed out a relevant formation of CO upon soot combustion by NO$_2$ in line with literature suggestions [34]; this indicates that Pt is involved in the CO oxidation since no appreciable CO evolution is observed at the reactor outlet. The involvement of NO$_x$ (and more specifically of NO$_2$) in the oxidation of soot is also pointed out by the fact that when the NO$_x$ storage is carried out in the absence of soot, a higher NO$_2$ formation is observed (see below). This points out that NO$_2$ is involved in the removal of soot, although the participation of the stored nitrates cannot be ruled out, as will be discussed below.

At the end of the NO$_x$ adsorption (lean phase), the gas feed is switched to rich conditions to regenerate the catalyst surface from the stored NO$_x$. Accordingly, 4000 ppm of H$_2$ have been fed to the reactor upon NO and oxygen shutoff. H$_2$ is completely consumed upon admission (see the insert of Fig. 1) and a simultaneous N$_2$ evolution is observed at the reactor outlet. The N$_2$ concentration reaches a level of about 800 ppm, in line with the stoichiometry of reaction (5):
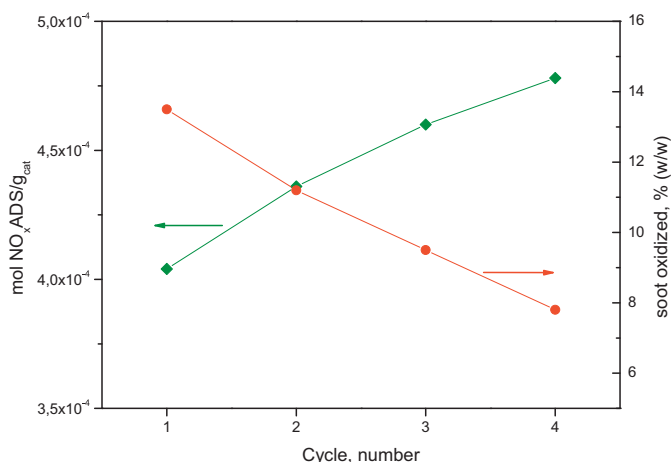
$$Ba(NO_3)_2 + 5H_2 + CO_2 \rightarrow BaCO_3 + N_2 + 5H_2O \qquad (5)$$
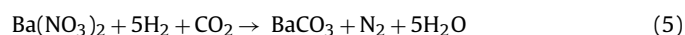
Fig. 2. Amounts of stored NO_x (mol/g_{cat}) and of soot oxidized (%, w/w) during lean–rich cycles at 350 °C over PtBa/Al_2O_3-soot mixture. Exp. conditions: see caption Fig. 1.

The N_2 concentration keeps almost constant for several seconds; then it decreases and a peak of NH_3 is observed, according to the stoichiometry of reaction (6):

$$Ba(NO_3)_2 + 8H_2 + CO_2 \rightarrow BaCO_3 + 2NH_3 + 5H_2O \qquad (6)$$
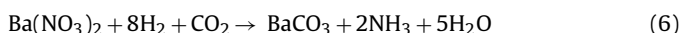
In line with the stoichiometry of reactions (5) and (6), a decrease of the CO_2 inlet concentration is observed, due to the formation of Ba carbonates at the expenses of the stored nitrates. The N_2 selectivity of the regeneration process is high, being near 95%. As detailed in previous studies [35–37], the observed sequence of reaction products has been explained on the basis of a two-step pathway involving at first the fast formation of ammonia upon reaction of nitrates with H_2 (reaction (6)), followed by the slower reaction of the so formed ammonia with the stored nitrates leading to the selective formation of N_2 (reaction (7)):

$$3Ba(NO_3)_2 + 10NH_3 \rightarrow 8N_2 + 3BaO + 15H_2O \qquad (7)$$

As discussed elsewhere [35–37], the observed temporal evolution of products during the reduction is due to the development of an H_2 front which travels along the reactor: NH_3 is initially formed in correspondence with the H_2 front, and reacts with NO_x stored downstream the front leading to N_2 evolution. Accordingly NH_3 evolution is observed at the reactor outlet after N_2 only when the nitrates are reduced and the H_2 front reaches the end of the catalyst bed.

The data described above clearly indicate that the catalyst system is able to simultaneously store/reduce NO_x and oxidize soot. However, considering the whole sequence of the four NO_x storage–reduction cycles (Fig. 1), it appears that the behavior of the PtBa/Al_2O_3 catalyst is affected by the residual soot loading. In fact the NO_x breakthrough progressively increases during the lean/rich sequence from ~100 s to ~140 s passing from the first to the fourth cycle, respectively, i.e. upon decreasing the soot loading. The increase in the dead time is accompanied by an increase of the amounts of NO_x stored up to steady-state, from 4.04×10^{-4} mol/g_{cat} for the first cycle to 4.78×10^{-4} mol/g_{cat} for the fourth cycle (Fig. 2).

Fig. 2 also shows the amounts of soot which is oxidized during the lean phase as a function of the cycle number, estimated from the amounts of evolved CO_2. During the lean phase of the first cycle, roughly 13% of the initial soot loading is oxidized, which reduces to 8% during the fourth cycle. At the end of the sequence the residual soot loading is near 3.9% (w/w). In fact the CO_2 concentration measured at steady-state at the end of the lean phase decreases from 1450 ppm of the first cycle to 1250 ppm of the fourth cycle, indicating a progressive decrease of the rate of soot combustion.

Of note, the NO_2 concentration is similar for all cycles during the whole experiment, as well as the NO/NO_2 ratio, although the progressive decrease of the soot combustion rate and the involvement of NO_2 in the oxidation of soot. These results are in line with our data discussed elsewhere [21] obtained during isothermal soot oxidation over PtBa/Al_2O_3 at 350 °C in presence of O_2 and NO and showing that the NO_2 concentration exhibits a remarkable increase only when the soot loading is very low (near 1%, w/w).

Finally, considering the reduction phase, no significant changes both in the products formation and in their temporal evolution are observed during the cycles. N_2 selectivity values near 95% have been calculated in lean/rich cycles, thus indicating a negligible effect of soot on the regeneration of the stored NO_x.

A comparison of the catalytic behavior of the PtBa/Al_2O_3 catalyst during a lean–rich cycle in the presence and in the absence of soot is shown in Fig. 3A and B, respectively (a concentration of 500 ppm of NO has been used during the lean phase). In the presence of soot (6.2% (w/w) in the case shown in Fig. 3A) a shorter dead time for NO_x breakthrough is observed during the lean phase (240 vs. 280 s); the amounts of NO_x stored at the end of the lean phase is also lower (3.8×10^{-4} vs. 4.9×10^{-4} mol/g_{cat}). Besides, a lower NO_2/NO ratio is measured in the presence of soot due to the involvement of NO_2 in the soot oxidation. On the other hand, no appreciable changes in the behavior of the sample during the rich phase are observed.

Soot is oxidized during the lean phase: as seen in Fig. 3A, the steady state level of the CO_2 concentration at the end of the lean phase is higher than the inlet value (1140 ppm vs. 1000 ppm), corresponding to a rate of soot oxidation of 1.04×10^{-8} mol/s. This value is lower than that observed in the case of the run carried out with 1000 ppm NO during the lean phase likely due to the lower NO_2 concentration observed with 500 ppm of NO in the feed [26].

In conclusions the results shown in Figs. 1–3 point out that the presence of soot affects the NO_x storage behavior of the investigated LNT system and in particular decreases the NO_x storage capacity of the catalyst, in line with the results reported in our previous works [23,25,26] and by other authors as well [27]. On the other hand the presence of soot does not impact significantly the catalyst behavior during the rich phase.

In order to investigate more in details the effect of soot on the behavior of the model PtBa/Al_2O_3 sample, lean–rich cycles have been performed at other temperatures, in the temperature range 200–350 °C, both in the absence and in the presence of soot. The results (here not reported for brevity) indicate that in the absence of soot the amounts of NO_x stored during the lean phase decrease upon decreasing the temperature from 5.6×10^{-4} mol/g_{cat} at 350 °C to 2.6×10^{-4} mol/g_{cat} at 200 °C. The presence of soot has a negative impact on the NO_x storage at all the investigated temperatures, in that it decreases the amounts of NO_x stored during the lean phase. Soot is oxidized during the lean phase, but soot oxidation is appreciable only at 300 °C and above.

Concerning the rich phase, it is noted that in the absence of soot the N_2 selectivity of the reduction process increases with temperature, as already pointed out in other studies and in line with the two-steps mechanism for NO_x reduction [35–37]. The presence of soot does not affect significantly the reduction process, as already observed at 350 °C (see above). These results parallels those obtained under different experimental conditions (lean and rich phases separated by an inert purge in between) and already reported elsewhere [26].

3.2. Soot reaction with adsorbed NO_x species: TPD experiments

3.2.1. PtBa/Al_2O_3 catalyst

To gain further insight into the effect of soot on the adsorbed NO_x species (nitrates) and in particular on their stability/reactivity, TPD experiments of the stored nitrates in the presence and in the
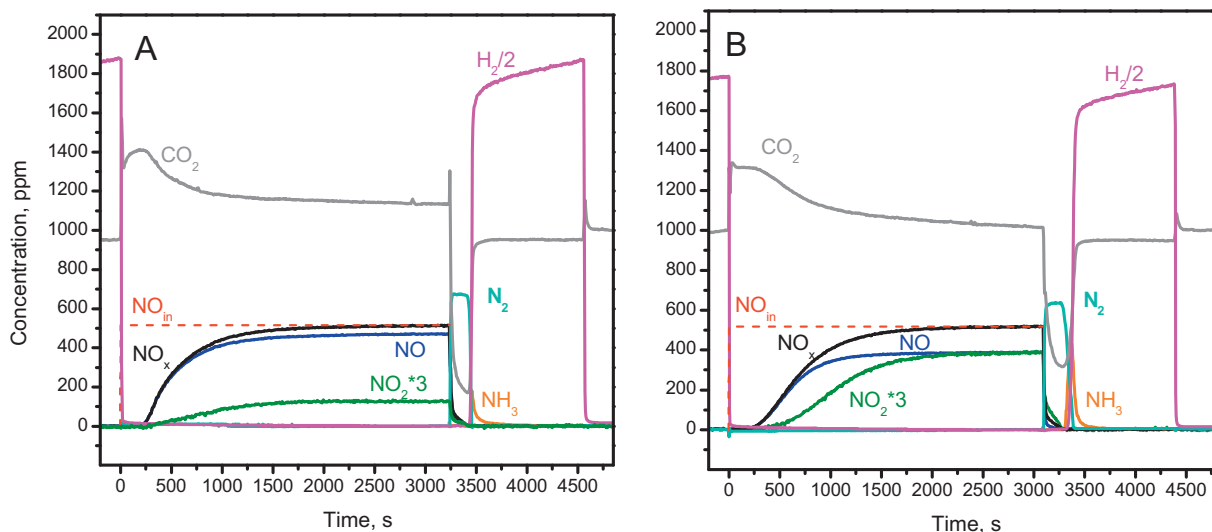
Fig. 3. Lean–rich cycles at 350 °C over PtBa/Al$_2$O$_3$ catalyst in the presence (A) and in the absence of soot (B). Lean phase: 500 ppm NO + O$_2$ (3%, v/v) in He, CO$_2$ (0.1%, v/v) and H$_2$O (1%); rich phase: 4000 ppm H$_2$ in He, CO$_2$ (0.1%, v/v) and H$_2$O (1%).
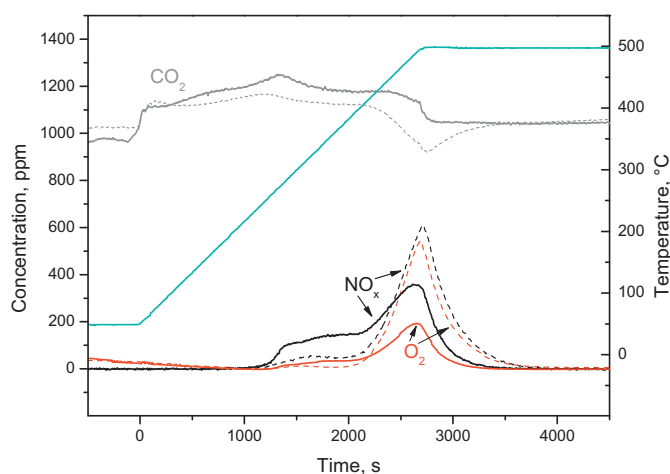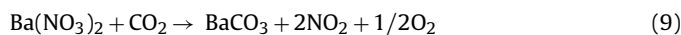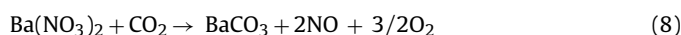

Fig. 4. TPD after NO$_x$ adsorption at 350 °C over PtBa/Al$_2$O$_3$ in the absence (dashed lines) and in the presence of soot (solid lines).

absence of soot have been carried out. Since soot affects the NO$_x$ storage on the PtBa/Al$_2$O$_3$ system, NO$_x$ have been stored at 350 °C in the absence of soot, and then the sample has been mixed with soot before the TPD runs (see Section 2), thus realizing a loose contact between soot and the nitrated catalyst. A reference TPD run has also been carried without mixing with soot.

The results of the TPD runs carried out the absence and in the presence of soot (dashed and solid lines, respectively) are shown in Fig. 4 in terms of NO$_x$, O$_2$ and CO$_2$ concentrations.

In the absence of soot (dashed lines) the nitrate decomposition is observed above 350 °C (i.e. the adsorption temperature), although very small amounts of NO$_x$ are also seen at lower temperatures. Nitrate decomposition occurs with evolution mainly of NO (along with minor amounts of NO$_2$) and of O$_2$. These results perfectly match those already published elsewhere [26] and confirm that the thermal stability of stored NO$_x$ is ruled by their adsorption temperature. The nitrate decomposition is not completed at the end of the heating rate at 500 °C, but is completed during the subsequent hold at this temperature. It is noteworthy that the overall amounts of evolved NO, O$_2$ and NO$_2$, estimated by integration of

the TPD peaks, are well in line with the stoichiometry of nitrates decomposition reactions (8) and (9):

$$Ba(NO_3)_2 + CO_2 \rightarrow BaCO_3 + 2NO + 3/2O_2 \qquad (8)$$

$$Ba(NO_3)_2 + CO_2 \rightarrow BaCO_3 + 2NO_2 + 1/2O_2 \qquad (9)$$

In fact the measured O/N atomic ratio in the evolved products (i.e. (NO + 2NO$_2$ + 2O$_2$)/(NO + NO$_2$)) is 2.6, very close to the theoretical value of 2.5.

Finally, a decrease of the CO$_2$ concentration (contained in the feed stream with a level of 1000 ppm) is observed in correspondence with the nitrate decomposition, due to the re-adsorption of CO$_2$ on the Ba sites leading to the formation of Ba carbonates at the expenses of Ba nitrates (reactions (8) and (9)).

Solid lines in Fig. 4 show the results of a TPD run performed in the presence of soot (i.e. after mixing the nitrated catalyst sample with soot). The decomposition of nitrates is shifted at lower temperatures if compared to the soot-free sample, in that a significant release of NO$_x$ is observed already in the temperature range 260–350 °C. The nitrate decomposition is then completed at higher temperatures, with NO$_x$ (only NO) and O$_2$ peaking near 485 °C. Besides, no a net CO$_2$ uptake is observed. It is suggested that in this case a surface reaction takes place involving nitrates and the soot particle:

$$C + Ba(NO_3)_2 \rightarrow BaCO_3 + 2NO + 1/2O_2 \qquad (10)$$
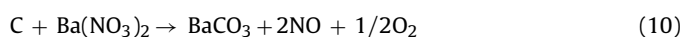
which results in the release of NO and O$_2$ and in the formation of carbonates whose formation accounts for the lack of a significant CO$_2$ net uptake from the gas phase in the TPD experiment with the catalyst/soot mixture.

These results clearly indicate that the presence of soot decreases the thermal stability of the stored nitrates. Moreover, if compared to the soot-free sample, a different distribution of the evolved products is also observed: in fact the calculated O/N atomic ratio of the gaseous products evolved during the entire TPD in the presence of soot is near 1.7, well below the stoichiometric O/N value of 2.5 for the nitrate decomposition. This indicates that nitrates and/or their decomposition products oxidize soot to CO$_2$, in line with the absence of a net CO$_2$ uptake (reaction (10)).

Based on the above observation, it clearly appears that soot promotes the decomposition of the NO$_x$ adsorbed species, which is in fact observed at lower temperature if compared to the soot-free sample. This calls for the existence of a surface reaction involving
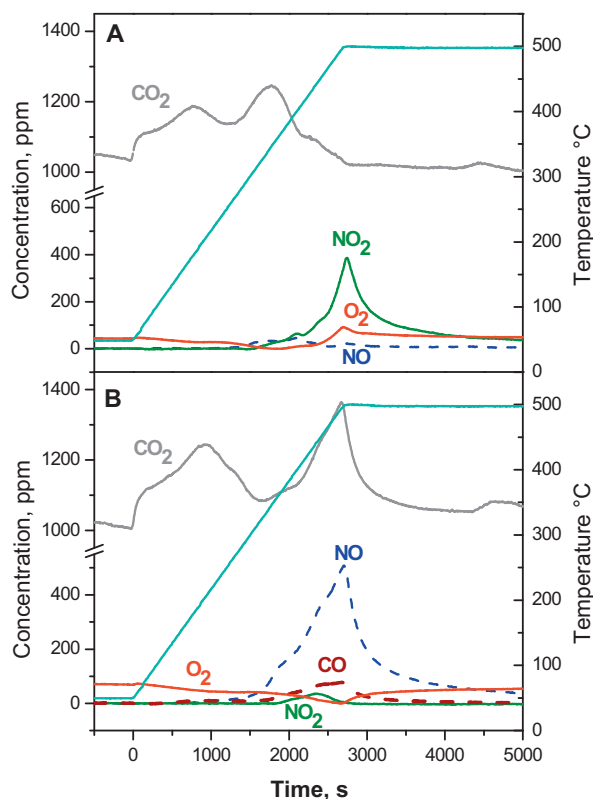
Fig. 5. TPD after NO_x adsorption at 350 °C over Ba/Al_2O_3 catalyst in the absence (A) and in the presence of soot (B).

the stored nitrates and the soot particles. As a matter of fact, studies on the reduction of the stored nitrates with several reductants suggested that nitrates are rather mobile on the surface [38,39], the driving force for the mobility of nitrates being the presence of reduced Pt sites (leading to nitrate decomposition/reduction). The role of the reductant in the process is to keep Pt in a reduced form. It is speculated that the soot particles, acting as reducing center for the NO_x species, provide the driving force for the process leading to nitrate reduction/decomposition (and soot oxidation). A similar nitrate destabilizing effect has been attributed to Pt in $PtBa/Al_2O_3$ catalysts, in order to explain the decrease in the decomposition temperature of nitrates which is observed upon Pt addition to Ba/Al_2O_3 [40].

3.2.2. Ba/Al_2O_3 catalyst

TPD runs over nitrated samples: In order to check whether Pt has a role in the soot-nitrate surface reaction, TPD experiments have been carried out over the binary Ba/Al_2O_3 catalyst in the absence and in the presence and of soot after NO_2 adsorption at 350 °C. The obtained results are shown in Fig. 5A and B (absence and presence of soot, respectively) in terms of concentration traces of the various evolved products (NO, NO_2, O_2, CO_2 and CO). In the case of the soot-free Ba/Al_2O_3 sample (Fig. 5A), nitrates decompose above 350 °C (i.e. the adsorption temperature) with evolution mainly of NO_2. Evolution of O_2 is also observed while that of NO is very small. Worth to note that in spite of the long isothermal period at 500 °C, nitrate decomposition is not yet completed at the end of the TPD run: in fact the NO_2 concentration shows a very long tail which extends for more than 4 h (not shown in the figure). At the end of the run, only a portion of the stored nitrates have been decomposed.

The TPD profile obtained in the presence of soot (Fig. 5B) is very different: the decomposition onset of the stored NO_x is observed near 300 °C, that is roughly 50 °C below that observed in the case of
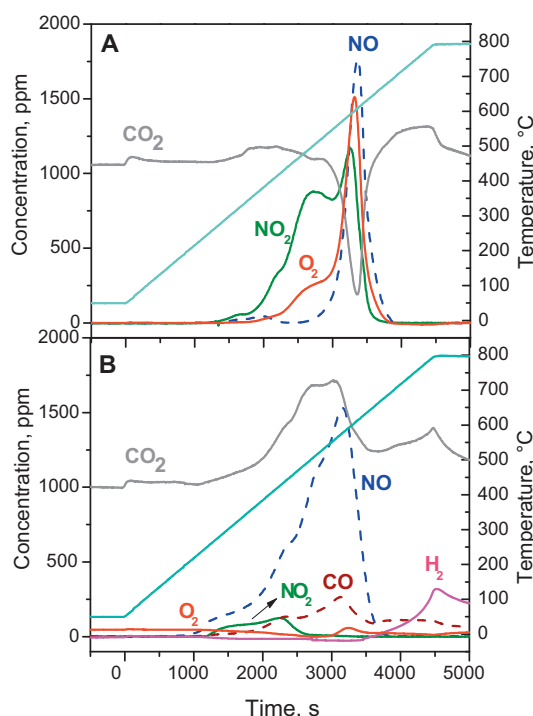
the soot-free sample, and is almost completed after the 4 h isothermal period at 500 °C. Also the distribution of the evolved products is different: in fact NO represents the major decomposition product and no significant amounts of NO_2 or O_2 are observed. Moreover, in correspondence with the NO evolution, a significant production of CO_2 is detected above the inlet value of 1000 ppm. Formation of significant amounts of CO (75 ppm) are also observed in this case, in line with other studies showing the formation of CO along with that of CO_2 during the non-catalytic soot oxidation by NO_2 [34].

These results indicate that the surface reaction between soot and the stored nitrates is not catalyzed by Pt: even in the absence of the noble metal, soot reacts with the NO_x ad-species which in fact decompose at lower temperatures if compared to the soot-free sample. This is in line with previous suggestions indicating that the soot particles may provide the driving force for nitrates mobility and their reduction/decomposition.

Effect of the soot/nitrate contact: To further investigate the interaction between soot and nitrates, and in particular the effect of the soot/nitrate contact, TPD experiments were performed with samples with a loose and a full contact between soot and the nitrates. In the first case (loose contact) nitrates were deposited over alumina by impregnation with an aqueous solution of $Ba(NO_3)_2$ ($Ba(NO_3)_2/Al_2O_3$ sample) followed by drying at 80 °C and gently mixing with soot; in the other case (full contact) the soot was directly impregnated with $Ba(NO_3)_2$ ($Ba(NO_3)_2/soot$ sample). The obtained results are shown in Figs. 6 and 7, where the heating ramp was ended at 800 °C.

In the case of the loose contact system, a reference TPD run was also carried without mixing the $Ba(NO_3)_2/Al_2O_3$ sample with soot (Fig. 6A). In this case the decomposition of the Ba nitrate species is apparent above 300 °C with the initial evolution of NO_2 (and O_2), showing a maximum near 500 °C. Then a decomposition peak centered near 600 °C is observed, accompanied by the evolution of NO, O_2 and NO_2. In correspondence with the nitrate decomposition a decrease of the CO_2 concentration is also observed, from the inlet value (1000 ppm) to a minimum of 200 ppm, due to readsorption for
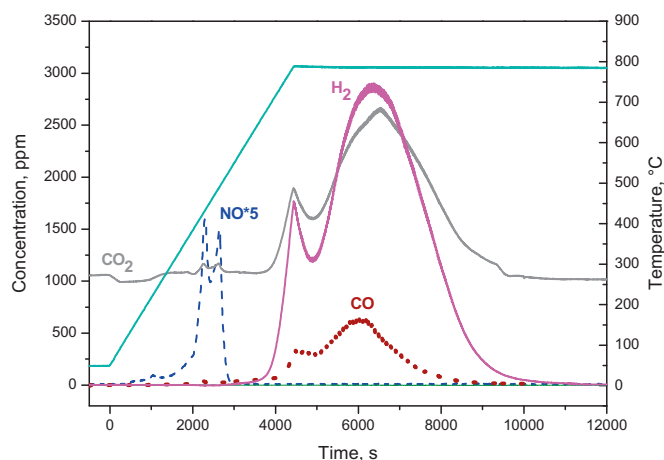

Fig. 6. TPD over $Ba(NO_3)_2/Al_2O_3$ catalyst in the absence (A) and in the presence of soot (B).

Fig. 7. TPD over $Ba(NO_3)_2$/soot "full contact" system.

carbonates formation onto the catalytic surface. Complete decomposition of the NO_x adsorbed species is achieved at temperatures slightly below 700 °C. This result is in line with the decomposition of nitrates formed upon NO_x adsorption (Fig. 5A); however in the case of Fig. 5A only the first NO_2 peak could be observed, since the heating ramp of the TPD run was limited at 500 °C.

A different picture is apparent in the presence of soot (Fig. 6B): the temperature onset for nitrate decomposition is observed near 230 °C, i.e. more than 70 °C below that of the soot-free system. The evolution of mainly NO is observed in this case, with much lower amounts of NO_2 and O_2. Besides, in correspondence with the NO evolution, a significant CO_2 production is observed, along with CO (maximum 260 ppm). These results resemble those obtained in the case of the sample obtained by NO_x adsorption (Fig. 5B) and confirm the capability of nitrates to oxidize soot at temperature well below that of their decomposition (being reduced to NO).

Finally, worth to note that in the presence of soot (Fig. 6B) the production of 300 ppm of H_2 is also evident at temperature above 700 °C, accompanied by the evolution of CO. This is due to the occurrence of the carbon gasification reaction (11):

$$C + H_2O \rightarrow CO + H_2 \tag{11}$$

due to the presence of water (1%, v/v) in the feed stream. CO_2 formation is also observed likely due to the occurrence of the water gas shift reaction (12):

$$CO + H_2O \rightarrow CO_2 + H_2 \tag{12}$$

The carbon gasification reaction is catalyzed by Ba, in line with the well known effect of alkaline/alkaline-earth oxides on this reaction [41,42]. In fact TPD experiments carried out over bare soot (here not shown) indicate that the carbon gasification reaction (11) takes place appreciably only at temperatures above 700 °C with very small production of CO and H_2.

The results of the TPD experiment carried out over the "full contact" sample is shown in Fig. 7. When $Ba(NO_3)_2$ is directly deposited onto soot (i.e. when an intimate contact is provided between nitrates and the soot particle) significant changes in the TPD profile are observed with respect to the loose contact sample (compare Figs. 7 and 6B). In fact in this case the temperature threshold for the nitrate decomposition significantly decreases with respect to that of the corresponding loose contact system (Fig. 6B), being NO evolution observed at temperatures as low as 150 °C. Moreover complete nitrate decomposition is obtained near 550 °C (vs. 700 °C of $Ba(NO_3)_2$/Al_2O_3-soot system). The production of CO_2 in correspondence with NO evolution points out also in this case the soot oxidation by the nitrates. Finally also in this case at temperature
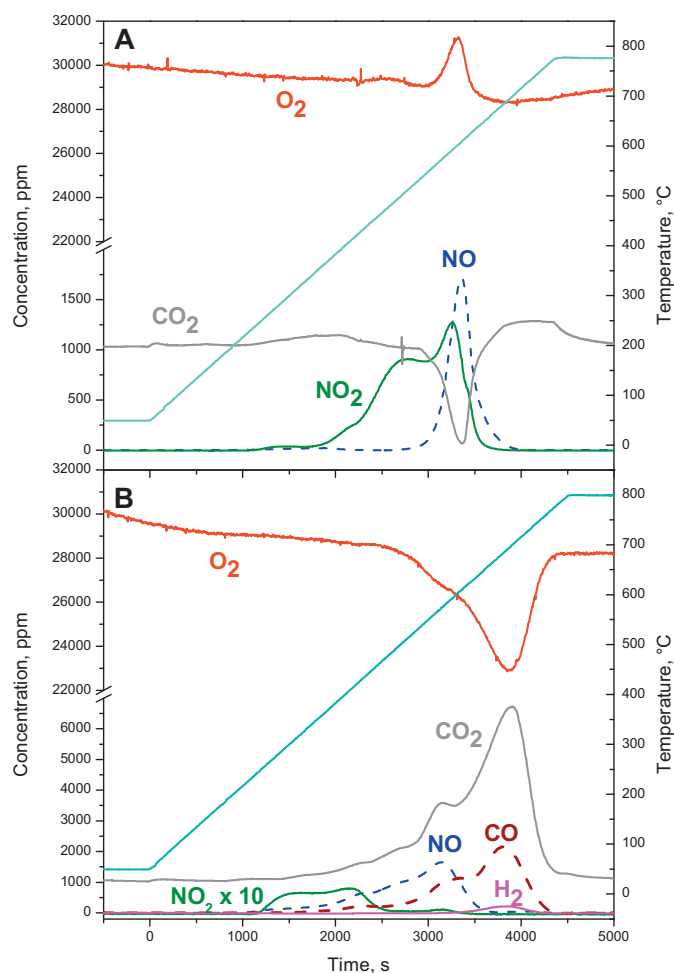

Fig. 8. TPO over $Ba(NO_3)_2$/Al_2O_3 catalysts in the absence (A) and in the presence of soot (B).

above 700 °C the simultaneous production of H_2, CO and CO_2 is observed due to the occurrence of reactions (11) and (12). Notably in this case a much higher soot gasification rate is measured: as matter of fact the maximum production of 3000 and 600 ppm is measured for H_2 and CO, respectively. The high H_2 and CO production is due to the catalytic effect of Ba (in close-contact with the soot) on the carbon gasification reaction.

Effect of the presence of oxygen: Finally, the effect of the presence of oxygen on the nitrate-soot interaction has also been addressed. For this purpose TPO runs have been performed with the $Ba(NO_3)_2$/Al_2O_3 sample in the absence and in the presence of soot, and results are shown in Fig. 8A and B, respectively. In the case of the soot-free sample (Fig. 8A), the results closely resemble those obtained during the TPD experiments (Fig. 6A), with nitrate decomposition apparent above 300 °C with the evolution of NO_2, NO and O_2, showing maxima near 500 °C and 600 °C, and the uptake of CO_2. These results show that the decomposition of the nitrates is not significantly affected by the presence of oxygen in the feed stream.

In the presence of soot (Fig. 8B), the temperature onset for nitrate decomposition is observed well below that of the soot-free system, like during the TPD experiment. Accordingly the soot-nitrate interaction is not significantly affected by the presence of oxygen. The evolution of NO is observed in this case, with much lower amounts of NO_2. Formation of CO_2 (and of CO as well) is also detected above 300 °C, with a maximum near 700 °C and a shoulder at 550 °C. The shoulder of the CO_x concentration at 550 °C is

associated with the soot oxidation by nitrates, whereas the maximum at 700 °C is due to soot oxidation by O_2 as confirmed by blank TPO experiments carried out in the absence of the catalyst (here not reported). Worth to note that a shoulder is observed at 550 °C in the O_2 concentration trace, corresponding to the maximum in the NO concentration and to the shoulder in the CO_2 concentration traces. This suggests the participation of O_2 also during the soot oxidation by nitrates, in line with literature reports showing the participation of O_2 during the soot oxidation by NO_x [43].

4. Conclusions

In the present study the interaction of soot with nitrates stored on a model PtBa/Al_2O_3 LNT catalyst sample has been investigated under realistic conditions, i.e. upon cycling under lean/rich conditions and in the presence of water and CO_2 in the feed stream. The results pointed out that the presence of soot decreases the NO_x storage capacity of the catalyst during the lean phase. The inhibiting effect of soot on the NO_x storage capacity increases with the soot amount, up to 11% (w/w) (the maximum investigated soot loading), and is observed at different temperatures in the range 200–350 °C. However, the presence of soot does not affect significantly the catalyst behavior during the rich phase, i.e. during the regeneration of the stored nitrates.

Simultaneously with the NO_x storage, at temperatures above 300 °C soot is oxidized to CO_2 during the lean phase. Soot oxidation occurs thorough the participation of NO_2 formed by NO oxidation on Pt sites; in fact the NO_2 concentration measured at the reactor outlet is significantly lower in the presence of soot than in its absence. However, in parallel with this NO_2-soot oxidation pathway, the participation of the stored nitrates in the soot oxidation is also likely. This has been shown by TPD/TPO experiments carried out over both the model PtBa/Al_2O_3 and Ba/Al_2O_3 samples in which the reactivity/thermal decomposition of nitrates has been investigated in the presence and in the absence of soot. Clear indication on the occurrence of a surface reaction involving soot and the stored nitrates has been pointed out, leading to soot oxidation (and nitrate reduction). In fact the stored nitrates are able to oxidize soot at temperatures well below those corresponding to their decomposition in the absence of soot. This reaction possibly involves the surface mobility of the stored nitrates, soot particles being the driving force for the process and acting as reduced centers. This process does not require the presence of the noble metal (Pt) in that it occurs in the case of the Ba/Al_2O_3 catalyst sample as well; as expected, it is favored by the contact between the nitrates and soot. In fact when nitrates are stored onto the soot, the nitrate/soot reaction is monitored at lower temperatures.

Acknowledgement

References

[1] T. Johnson, Platinum Met. Rev. 52 (2008) 23.
[2] B.A.A.L. van Setten, M. Makee, J.A. Moulijn, Catal. Rev. 43 (4) (2001) 489.
[3] A. Güthenke, D. Chatterjee, M. Weibel, B. Krutzsch, P. Kocˇí, M. Marek, I. Nova, E. Tronconi, Adv. Chem. Eng. 33 (2008) 103.
[4] P. Forzatti, Appl. Catal. A: Gen. 222 (2001) 221.
[5] W.S. Epling, L.E. Campbell, A. Yezerets, N.W. Currier, J.E. Parks, Catal. Rev. Sci. Eng. 46 (2004) 163.
[6] S. Matsumoto, Catal. Today 90 (2004) 183.
[7] S. Roy, A. Baiker, Chem. Rev. 109 (2009) 4054.
[8] L. Lietti, G. Ramis, F. Berti, G. Toledo, R. Robba, G. Busca, P. Forzatti, Catal. Today 42 (1998) 101.
[9] L. Xu, R. McCabe, W. Ruona, G. Cavataio, SAE Technical Paper, 2009-01-0285 (2009).
[10] A. Lindholm, H. Sjövall, L. Olsson, Appl. Catal. B: Environ. 98 (2010) 112.
[11] P. Forzatti, L. Lietti, Catal. Today 155 (2010) 131.
[12] M. Weibel, N. Waldbüßer, R. Wunsch, D. Chatterjee, B. Bandl-Konrad, B. Krutzsch, Top. Catal. 52 (2009) 1702.
[13] E.C. Corbos, M. Haneda, X. Courtois, P. Marecot, D. Duprez, H. Hamada, Catal. Commun. 10 (2008) 137.
[14] E.C. Corbos, M. Haneda, X. Courtois, P. Marecot, D. Duprez, H. Hamada, Appl. Catal. A: Gen. 365 (2009) 187.
[15] K. Nakatani, S. Hirota, S. Takeshima, K. Itoh, T. Tanaka, SAE Paper SP-1674 2002-01-0957 (2002).
[16] J. Suzuki, S. Matsumoto, Top. Catal. 28 (2004) 171.
[17] J.A. Sullivan, O. Keane, A. Cassidy, Appl. Catal. B: Environ. 75 (2007) 102.
[18] A.L. Kustov, M. Makkee, Appl. Catal. B: Environ. 88 (2009) 263.
[19] C.-N. Millet, R. Chédotal, P. Da Costa, Appl. Catal. B: Environ. 90 (2009) 339.
[20] H. Lin, Y. Li, W. Shangguan, Z. Huang, Combust. Flame 156 (2009) 2063.
[21] L. Castoldi, R. Matarrese, L. Lietti, P. Forzatti, Appl. Catal. B: Environ. 64 (2006) 25.
[22] R. Matarrese, L. Castoldi, L. Lietti, P. Forzatti, Top. Catal. 42–43 (2007) 293.
[23] R. Matarrese, L. Castoldi, L. Lietti, P. Forzatti, Top. Catal. 52 (2009) 2041.
[24] R. Matarrese, L. Castoldi, L. Lietti, P. Forzatti, Catal. Today 136 (2008) 11.
[25] L. Castoldi, N. Artioli, R. Matarrese, L. Lietti, P. Forzatti, Catal. Today 157 (2010) 384.
[26] N. Artioli, R. Matarrese, L. Castoldi, L. Lietti, P. Forzatti, Catal. Today 169 (2011) 36.
[27] I.S. Pieta, M. García-Diéguez, C. Herrera, M.A. Larrubia, L.J. Alemany, J. Catal. 270 (2010) 256.
[28] B.S. Sánchez, C.A. Querini, E.E. Miró, Appl. Catal. A: Gen. 366 (2009) 166.
[29] B.S. Sànchez, C.A. Querini, E.E. Miró, Appl. Catal. A: Gen. 392 (2011) 158.
[30] N. Miyoshi, T. Tanizawa, K. Kasahara, S. Tateishi, European Patent Application 0 669 157 A1, 1995.
[31] A. Setiabudi, M. Makee, J.A. Moulijn, Appl. Catal. B: Environ. 50 (2004) 185.
[32] L. Castoldi, R. Matarrese, L. Lietti, P. Forzatti, Appl. Catal. B: Environ. 90 (2009) 278.
[33] F. Prinetto, G. Ghiotti, I. Nova, L. Castoldi, L. Lietti, E. Tronconi, P. Forzatti, Phys. Chem. Chem. Phys. 5 (2003) 4428.
[34] B.R. Stanmore, V. Tschamber, J.-F. Brilhac, Fuel 87 (2008) 131.
[35] L. Lietti, I. Nova, P. Forzatti, J. Catal. 257 (2008) 270.
[36] I. Nova, L. Lietti, P. Forzatti, Catal. Today 136 (2008) 128.
[37] P. Forzatti, L. Lietti, I. Nova, Eng. Environ. Sci. 1 (2008) 236.
[38] R.D. Clayton, M.P. Harold, V. Balakotaiah, C.Z. Wan, Appl. Catal. B: Environ. 90 (2009) 662.
[39] D. Bhatia, M.P. Harold, V. Balakotaiah, Catal. Today 151 (2010) 314.
[40] I. Nova, L. Castoldi, L. Lietti, E. Tronconi, P. Forzatti, SAE Technical Papers, 2006-01-1368, 2006.
[41] D.W. MacKee, Fuel 62 (1983) 170.
[42] D.W. MccKee, C.L. Spiro, P.G. Kosky, E.J. Lamby, Fuel 64 (1985) 805.
[43] F. Jacquot, V. Logie, J.F. Brilhac, P. Gilot, Carbon 40 (2002) 335.